

Monitoring of Multicell Converter and DC Motor

Nabila Adjissi^{1, *} and Belkacem Sait²

Abstract—This paper presents a hybrid sliding mode control of a multicell power converter. It takes into account the hybrid aspect of the conversion structure which includes the converter continuous and discrete states. The idea is based on using a hybrid control and an observer-type sliding mode to generate residuals from the observation errors of the system by including different types of faults in the transition between modes. The case when a DC motor is coupled to the multicell converter is also considered. In this case, it is shown that under certain admissible assumptions, the voltages across the capacitors and the speed of the motor can be acceptably estimated. The simulation results are presented at the end to illustrate the performance of the proposed approach using stateflow in sumulink (matlab). The developed method is illustrated in an example of the DC motor supply via a three cell converter which is a real example of an SDH characterized by continuous and discrete variables.

1. INTRODUCTION

Power electronics have been evolving through the last decade due to the development of semiconductor power components and new systems of energy conversion [1].

Among these systems, multicellular converters, which appeared at the beginning of the 1990s [2, 30], are based on the association in series of the elementary cells of commutation. During the last decade, these systems have become more and more attractive to industrial applications, especially in high-power applications [3].

Moreover, modeling is a very important step for control laws and observers synthesis. In literature, several approaches have been considered to develop methods of control and observation of multicell converters. Initially, models have been developed to describe their instantaneous [4], harmonic [5], or averaging [6] behaviors.

To benefit as much as possible from the large potential of the multicellular structure, an appropriate distribution of the voltages crossing each cell is needed.

These voltages are generated when a suitable control of switches is applied in order to obtain a specific value. The control of switches allows to cancel the harmonics at the switching frequency and to reduce the ripple of the chopped [11]. Some control laws have been proposed [8] and [9].

Anyway, the knowledge of capacitor voltages is always needed. Furthermore, it is important to note that the use of physical extra sensors in order to measure such voltages increases the cost and complexity of the system. That is why its estimation by means of an observer becomes an attractive and economical solution.

Different observer based methods have been developed for nonlinear systems such as [7] which talks about the sliding mode control, adaptive observers [21], observers by input-output injection [10], higher order sliding mode observers or finite time observers [16].

Both DC and AC motors have been extensively used in control systems, but each has its own characteristics. The main advantages of DC motors are easy control and wide adjustable range.

Received 11 September 2019, Accepted 8 February 2020, Scheduled 10 March 2020

* Corresponding author: Nabila Adjissi (adjissi.laig@gmail.com).

¹ Laboratory of Automatics and Informatics of Guelma, Department of Electrical Engineering, University of Setif1, Algeria.

² Automatic Laboratory of Setif, Department of Electrical Engineering, University of Setif1, Algeria.

Therefore, DC motors are often used in a variety of industrial applications such as robotic manipulators, where a wide range of motions are required to follow a predetermined trajectory under variable load [22].

In literature, many researches try to find a solution for the problem of observability of a hybrid system such as [26], from these solutions the sliding mode observer to control a DC motor [11], fault tolerant control for multicell converter four quadrants drive, [12, 13] binary control of converter [14], adaptive-gain second-order sliding mode observer [15], robust finite time observer [16, 17], adaptive observer for multicell chopper [18, 19].

For the first-order sliding modes, it is common to deal with the issues of stability, robustness, and convergence rate of the equilibrium by means of a Lyapunov approach [20]. For higher sliding mode and finite-time observers, the proof of stability is usually done using geometric homogeneity-based methods. Hence, the estimation of the convergence time and the study of robustness properties may be problematic in [16].

In this paper, multicellular converter can be used as a power interface between a sliding mode type control and a DC motor. We have used stateflow matlab to show the good functioning and to also show the faults that can happen when the program is running; for example a transitions fault or the transition blocked in the same mode which can be problematic must be salved.

2. SYSTEM MODELING

2.1. State Representation

The multicell converter consists of a series combination of p elementary switching cells and one cell being composed of two complementary switches. It has secondary sources produced by floating capacitors showing in Figure 1 [9]. It is a variable structure system that changes during operation. It is characterized by the choice of supply voltage E and a switching logic. Compared to conventional converters, it provides a greater number of voltage levels and reduces the harmonic content of the output signals. In comparison, a conventional inverter (H-bridge) is a converter which has two cells providing only two voltage levels. This structure has additional advantages: the possibility of modular construction and the use of components of general circulation. Safety and proper operation of the power converter are directly dependent on the proper distribution of voltages across each cell [25, 23]. Therefore, it is very important to ensure the balance of the voltages across floating capacitors. The characteristics of the converter ensure this balance by acting directly on the control signals of its switches.

The system includes discrete variables (control of semi-conductor components) and continuous ones (building tension, current, and voltage output). A modeling representation of hybrid state can be used.

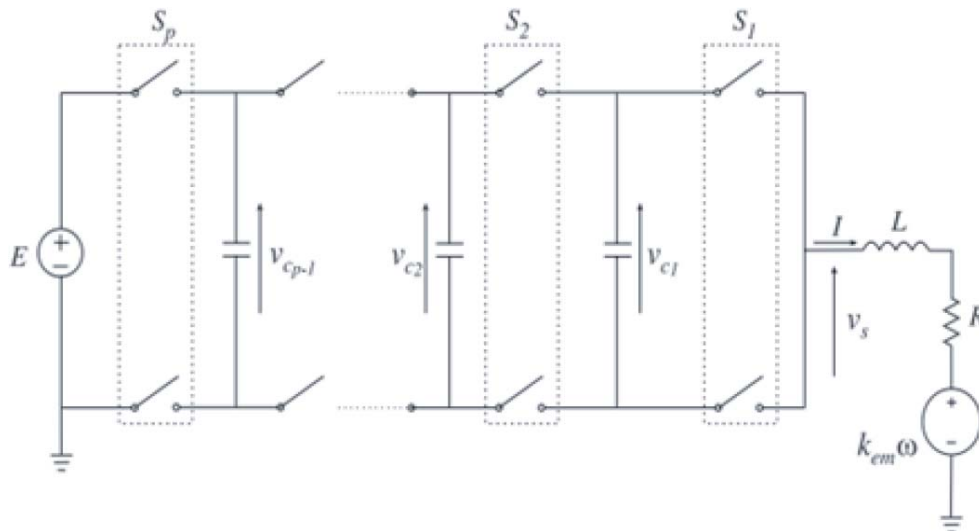


Figure 1. Topology of a converter with p independent commutation cells connected to a DC motor.

The behavior of multicell converter associated with a DC motor is governed by the following differential equations:

$$\begin{cases} T_u(t) = T_m(t) - T_p \\ j \\ T_m(t) = k_{em} \\ T_r(t) = f \\ T_p = Cte \end{cases} \quad \begin{cases} \dot{w}(t) = T_u(t) - T_r(t) \\ I(t) \\ w(t) \end{cases} \quad (1)$$

with

$$\begin{cases} T_m : \text{motor torque} \\ T_r : \text{resistant torque} \\ T_u : \text{useful torque} \\ T_p : \text{torque loss} \end{cases}$$

and

$$\begin{cases} \dot{I}(t) = -\frac{R}{L}I(t) + \frac{E}{L}u_p - \frac{k_{em}}{L}w(t) - \sum_{i=1}^{p-1} \frac{V_{ci}(t)}{L} (u_{i+1} - u_i) \\ \dot{V}_{cj}(t) = \frac{I}{c_i} (u_{i+1} - u_i) \\ \dot{w}(t) = \frac{k}{j}I(t) - \frac{f}{j}w(t) - T_p \\ y(t) = I(t) \end{cases} \quad (2)$$

where I is the load current, R the resistance, L the inductor, c_i the i th capacitor, V_{ci} the voltage of the i th capacitor, and E the voltage of the source. w , k , k_{em} , f , and j represent respectively the speed, electromechanical coefficient torque, constant of motor, generally $k_{em} = k$, the viscosity coefficient, and the total inertia of the DC motor, and u_i is the switch states.

$S \in \{0, 1\}$ is the signal for controlling the switches of the i th cell. The control signal S_i is equal to 1 when the switch of the upper part of the i th cell is conductive and equal to 0 when it is on the contrary. The output voltage can be expressed by the following relationship:

$$V_s = E \cdot S_p + \sum_{i=1}^{p-1} V_{ci} (S_i - S_{i+1})$$

A multicellular converter with p cells is defined with 2^p switching modes and $(p + 1)$ voltage levels available at the output.

Each cell i must support $V_{ci} - V_{ci-1}$ voltage for $i = (1, \dots, p - 1)$. To obtain a fair distribution power of voltage on each cell $(p - 1)$ references are chosen such that:

$$V_{ciref} = i \frac{E}{p}, \quad i = 1, \dots, p - 1$$

Assuming that only the load current I can be measured, it is easy to represent systems 1 and 2 as a hybrid system. The dynamics of the converter is given by:

$$\begin{cases} \dot{x} = A(u)x + B(u) \\ y = Cx \end{cases} \quad (3)$$

where $x = [I, V_{c1}, \dots, V_{cp-1}, w]^T$ is the continuous state vector, and $u = [u_1, u_2, \dots, u_p]^T$ is the switching control signal vector which takes only discrete values. The matrices $A(u), B(u), C$ are defined as:

$$A(u) = \begin{bmatrix} -\frac{R}{L} & -\frac{u_1}{L} & \dots & -\frac{u_{p-1}}{L} & \frac{k}{L} \\ -\frac{u_1}{C_1} & 0 & \dots & 0 & 0 \\ \vdots & \vdots & \dots & \vdots & \vdots \\ \frac{u_2}{C_2} & 0 & \dots & 0 & 0 \\ -\frac{f}{j} & 0 & \dots & 0 & \frac{k}{j} \end{bmatrix}$$

$$B(u) = \left[\frac{E}{L} u_p \ 0 \dots 0 \right]^T$$

$$C = [1 \ 0 \dots 0]$$

After we represent the system with the differential equations, we will use the hybrid automata for the graphic modeling.

2.2. Hybrid Automata Modeling of Three Cells Converter

A hybrid automata is presented basically as a finite state of automat with differential equations associated with its discrete states. Thus, the overall condition of a hybrid automata, at a given time, is defined by a pair (q, X) . q represents the status (discrete status) and X the value of the state vector. This global state is changed for two reasons. Crossing a discrete transition, which abruptly changes the situation and then often the evolution of the continuous state or directly the value of the state (jump). This crossing happens on the occurrence of an appropriate event and/or if an event condition becomes true; the temporal evolution affects X according to the differential equation associated with the current situation. This situation remains unchanged [28, 27].

The advantage of this representation is its simplicity. Describing unambiguously possibility of System Dynamic Hybrid (SDH) developments, it will be the basis of the analysis to establish formal properties. At every moment, a single discrete state is active, so there is only one set of equations (one continuous model). The hybrid nature is marked by the fact that a discrete event may cause the change of state, so switching the equations, but reaching a threshold value on a continuous variable can also lead to a change of discrete state.

The hybrid system is completely described by eight elements as follows [25, 27]: $\{Q, X, Init, F, Xq, H, G, R\}$ with

- $Q = \{q_1, q_2, q_3, \dots, \}$ the set of discrete states.
- $X = R^n$ are continuous states.
- $Init \subset Q \times X$ is a set of possible initial conditions.
- $F_{(\cdot)}(\cdot) : Q \times X \rightarrow R^n$ is the vector field associated with each discrete state; $F_q(X) = A(q)X + b(q)$.
- $Xq : Q \rightarrow P(X)$ associates with an invariant field for the discrete state q .
- $H \subset Q \times Q$ is the set of possible transitions in the automata $(T_{i,j})$.
- $G : H \rightarrow 2X$ the constraint in the continuous field for validating a transition e and H , with e being one possible transition.
- $R : G(e) \rightarrow P(X)$ is the reinitialization relation of continuous variables at the time of a discrete transition.

2.3. Application of Hybrid Automata for the Three Cells Converter

We distinguish eight modes given by $Q = \{q_1, q_2, \dots, q_8\}$, and each mode is defined in the space $X_{q_i} \in R_3$, $q_i \in Q$, where $x = [V_{c1}, V_{c2}, I, w]^T$ is the state vector of the system. The transitions T_{ij} have been derived in order to bring the state vector X inside a prescribed region around desired references $X_{ref} = [V_{ref1} \ V_{ref2} \ I_{ref} \ w_{ref}]^T$. With initial values $X_0 = [0 \ 0 \ 0 \ 0]^T$ and initial state $Q_0 = q_8$ as shown in the following Figure 2 [24, 27], we can resume the initial form of the system.

Table 1 gives different values of switches and different possible configurations, called mode q_i .

After modeling, diagnosis must take place using an observer in the first place and the faults detection in the second place.

2.4. Diagnosis the Fault in Cell Converter

The approach is based on using the observer of sliding mode to detect and isolate fault cell type. To generate the residuals, we begin with determining the dynamic behavior of the state variables of the converter, then they are compared to those obtained by the observer [10, 11].

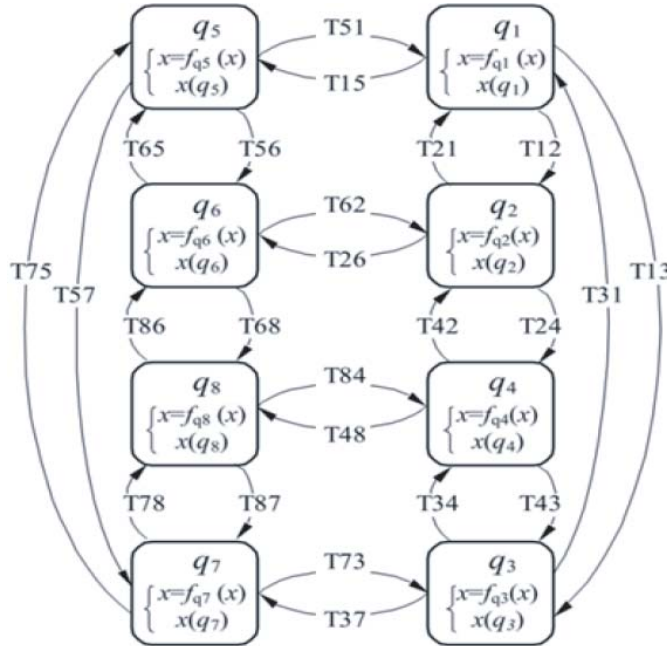


Figure 2. Hybrid automata for three cells converter.

Table 1. The different states of cells.

Mode q_i	u_3	u_2	u_1
q_1	0	0	0
q_2	0	0	1
q_3	0	1	0
q_4	0	1	1
q_5	1	0	0
q_6	1	0	1
q_7	1	1	0
q_8	1	1	1

2.5. Application of Sliding Mode

Studies show that we cannot have the observability of floating voltages V_{c1} and V_{c2} at the same time for the three cell converter, so the instantaneous model is not valid for building an observer that can reconstruct state variables of the converter. To remedy the problem of observability, we use a compact model of the converter so that the system can be observable [10]. Therefore, we talk about an observer based on sliding mode [31]. The principle of the latter is to force the dynamics of a system of order n to converge to an interval, called sliding surface [27].

In the case of observer of sliding mode, the dynamics concerned are those of the errors of observation $\tilde{X} = \hat{X} - X$. From their initial values $\tilde{X}(0)$, these errors converge to the equilibrium values in two steps:

In the first step, the path of the observation errors move towards the sliding surface on which the error between the output of the observer and the output of the real system (measurement) $\tilde{y} = \hat{y} - y$ are zero. This step, which is usually very dynamic, is called reaching mode.

In the second step, the trajectories of the observation errors slide on the sliding surface defined by $\tilde{y} = 0$. This later mode is called sliding mode [25].

Using the general compact form of a three cell converter, we can construct the observer that takes

the set of observation equations:

$$\begin{cases} \dot{\hat{X}}_i(t) = A(q_i)\hat{X}_i(t) + \hat{B}_i(q, u, \hat{y}) + H_i(q, \hat{X}) + \Phi_i(y - \hat{y}) \\ \hat{y}(t) = C\hat{X}_i(t), \quad i = 1, 2 \end{cases} \quad (4)$$

$p = 3; q_1 = u_2 - u_1, q_2 = u_3 - u_2; C = [0 \ 1 \ 0]$

where $\hat{X}_i = \begin{bmatrix} \hat{V}_{ci} \\ \hat{I} \\ \hat{w} \end{bmatrix}$; $A(q_i) = \begin{bmatrix} 0 & 0 & 0 \\ \frac{-q_i}{L} & 0 & 0 \end{bmatrix}$; $H_i(q, x) = \frac{1}{L} \begin{bmatrix} 0 & \sum_{j=1, j \neq i}^{p-1} q_j \hat{V}_{cj} \end{bmatrix}$ and $\hat{B}_i(q, u, \hat{y}) = \begin{bmatrix} \frac{q_i}{L} \hat{I} + \frac{E}{L} u_3 - \frac{k}{L} \hat{w} \\ \frac{k}{j} \hat{I} - \frac{f}{j} \hat{w} \end{bmatrix}$.

The gain of observation is written as $\lambda = [\lambda_1 \ \lambda_2 \ \lambda_3]^T$, $S = (I - \hat{I})$ is the switching surface.

$$\begin{cases} \dot{\hat{V}}_{c1} = q_1 \frac{\hat{I}}{c_1} + \lambda_1 \text{sign}(I - \hat{I}) \\ \dot{\hat{V}}_{c2} = q_2 \frac{\hat{I}}{c_2} + \lambda_2 \text{sign}(I - \hat{I}) \\ \dot{\hat{I}} = -\frac{R}{L} \hat{I} - \frac{k_{em}}{L} \hat{w}(t) - q_1 \frac{\hat{V}_{c1}}{L} - q_2 \frac{\hat{V}_{c2}}{L} + \frac{E}{L} u_3 + \lambda_3 \text{sign}(I - \hat{I}) \\ \dot{\hat{w}}(t) = \frac{k}{j} \hat{I}(t) - \frac{f}{j} \hat{w}(t) + \lambda_4 \text{sign}(I - \hat{I}) \end{cases} \quad (5)$$

we have $\begin{cases} \lambda_1 = \frac{\lambda_3}{\tau} L (u_2 - u_1) \\ \lambda_2 = \frac{\lambda_3}{\tau} L (u_3 - u_2) \\ \lambda_3 > |\Delta f_3|_{\max} \end{cases}$ with $\Delta f = f(\hat{x}, u) - f(x, u)$.

The goal of the gain λ_3 is to ensure the attractivity of the sliding surface. During this time interval, the intermediate voltage observed remains unchanged.

Gains λ_1 , λ_2 , λ_3 and λ_4 are given in order to impose the dynamics of the error of observation in sliding mode [13]. The theoretical dynamics of evolution of the tension with terminals of the floating capacitor depends on the current of maximum loading, and the value of the latter is:

$$\frac{dv}{dt} = \frac{|I|_{\max}}{C} \quad (6)$$

The time-constant τ must be fixed at

$$\tau = \frac{\lambda_3 L}{dv/dt} \quad (7)$$

It is noted that capacitors voltages and load current converge quickly towards their actual values. However, the convergence of the capacitors voltages is slower than load current [29]. The sliding surface converges consequently towards zero and remains there.

2.6. Residual Generation

The main idea is to generate residues which reflect inconsistencies between operation of nominal and defective system. Defects are present when the distribution of residual sequence is changed. In this case, one residue will be used only to detect a possible blockage (On and off) of switches [25, 11, 13].

$$R = \left\| \sum_{i=1}^n \frac{\Delta X_i}{X_{ref}} \right\| \text{ with } n = 4$$

And $\begin{cases} X_i = [V_{c1} - V_{c1_{obs}} V_{c2} - V_{c2_{obs}} I - I_{obs} w - w_{obs}] \\ X_{ref} = [V_{ref1} V_{ref2} I_{ref} w_{ref}] \end{cases}$

$$\text{then : } R = \left\| \frac{\Delta V_{c1}}{V_{ref1}} + \frac{\Delta V_{c2}}{V_{ref2}} + \frac{\Delta I}{I_{ref}} + \frac{\Delta w}{w_{ref}} \right\| \tag{8}$$

$$\text{if } \begin{cases} R = 0 \text{ there is no fault} \\ R \neq 0 \text{ there is a fault} \end{cases} \tag{9}$$

Figure 3 gives the diagram of fault generation and detection in a multicell converter. The faults F_i are affected in residue generation.

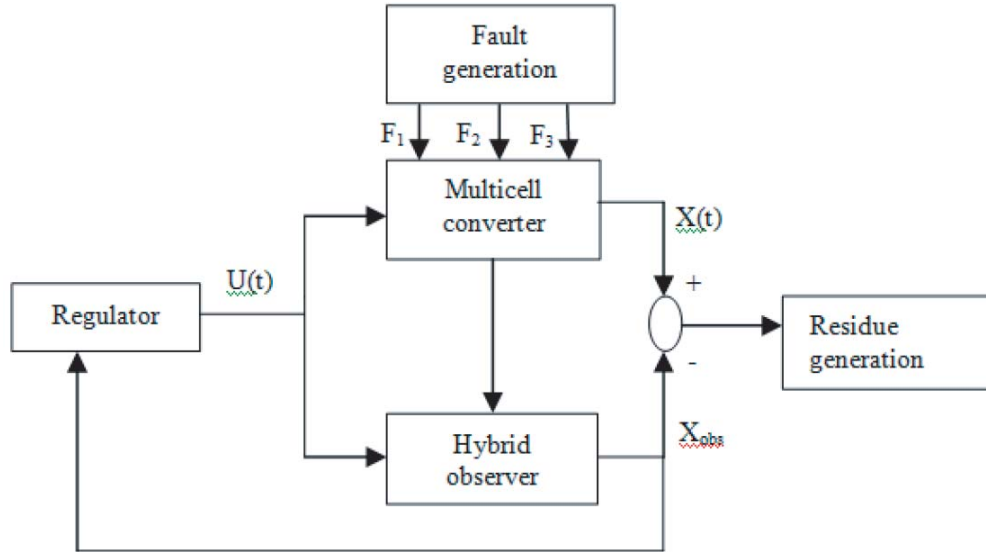


Figure 3. Block diagram of fault generation and detection in multicell converter.

3. SIMULATION RESULTS

The system is constitute by a three cell converter, with two load capacitors associated with DC motor, which is represented by a resistance R , an inductance L , and an electromagnetic force e . Table 2 shows the used parameters.

Table 2. The deferent system of parameters.

R	1.8Ω
L	1.5 mH
E	30 V
k	1.58 NmA
f	5 Nm/rd/s
j	$79\text{e-}8 \text{ kgm}^2$
$C_1 = C_2$	$40 \mu\text{F}$
V_{ref1}	10 V
V_{ref2}	20 V
I_{ref}	12 A
T_p	0 s

3.1. Functioning without Fault

For a simulation time $t = 0.3 \text{ s}$. The results of simulation are show in Figures 4 and 5.

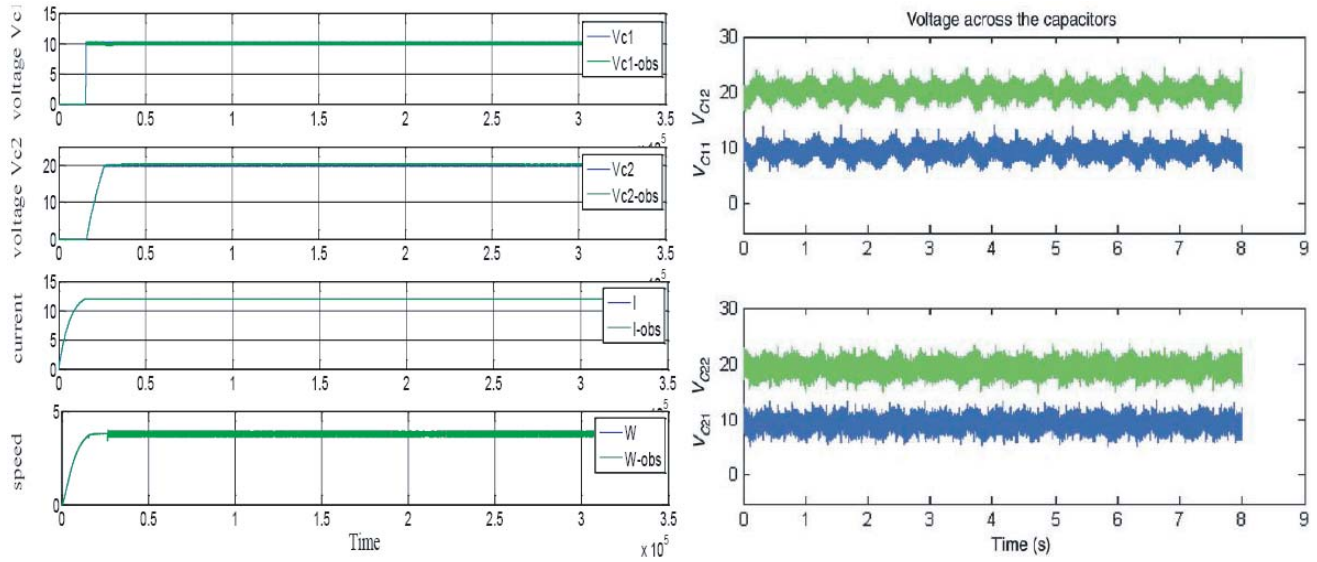


Figure 4. Evolution of state variables of the converter observed. We notice that we have obtained the same results as the work done in [11].

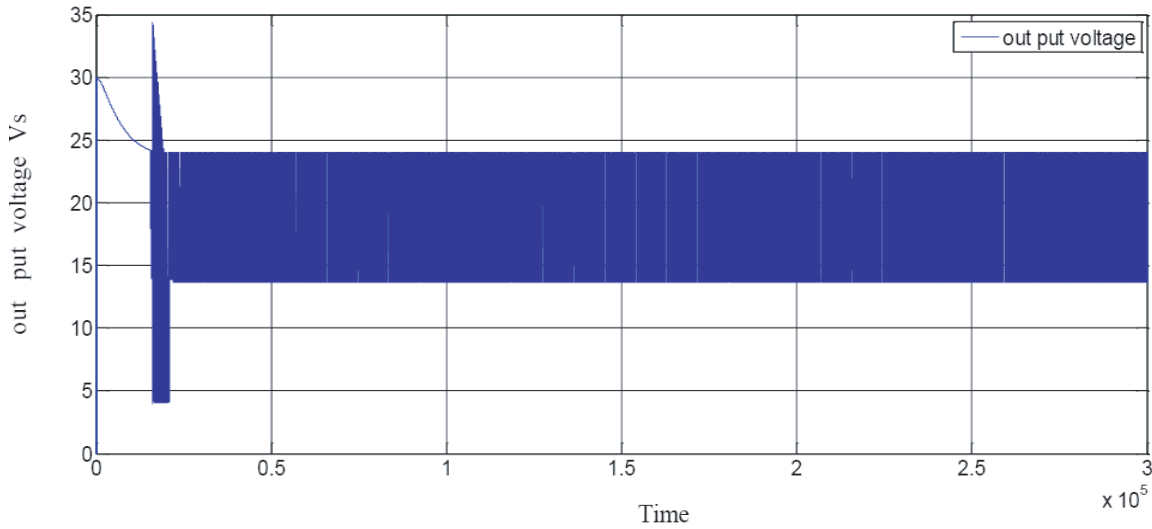


Figure 5. Evolution of output voltage V_s .

Figure 6 shows the evolution of the residue signal which converges to zero showing the reliability of the observer used.

3.2. Functioning with Fault

The approach is based on the use of an observer for detecting and locating the faulty cell; therefore, we must test every possible case of errors between the estimated variables and the system exits, which is a residue generator. Table 3 gives the effects blocking switches on the states of the system.

3.3. Fault Discrete of System Functioning

There are three possible scenarios for a fault:

- Blocked of a switch;

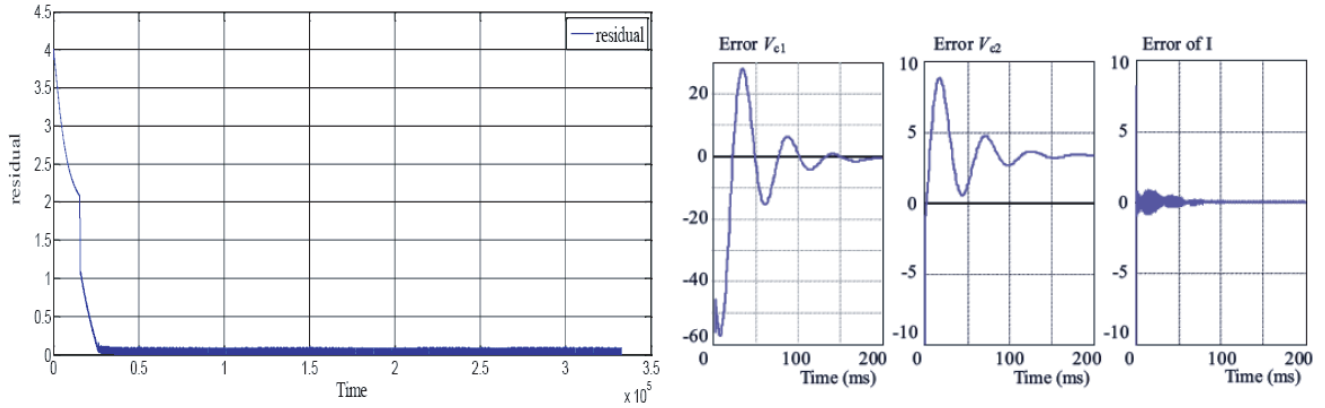


Figure 6. Evolution of the residual R , the residue is zero in the absence of fault [25].

Table 3. Signature of operation with fault for blocking switches.

blocking switches		Effects on the states of the system			
		V_{c1}	V_{c2}	I	w
u_1	1	↓	↓	↑	↑
	0	↑	↑	↓	↓
u_2	1	↑	↓	↑	↑
	0	↓	↑	↓	↓
u_3	1	↑	↑	↑	↑
	0	↓	↓	↓	↓

with: \downarrow : { decrease.
 \uparrow : { increase.

- Non transition,
- Transition to a non successor mode.

3.4. Blocked of a Switch

For example, the blocked switch, $u_3 = 0$, and the hybrid automata model of the converter will be reduced to 4 modes. The introduction of the blocking of $u_3 = 0$ from $t = 0.1$ s to $t = 0.2$ s gives the results of simulation as follows. Figure 7 shows the evolution of the state variables of the converter, and Figure 8 shows the evolution of the output voltage V_s . Figure 9 presents the evaluation of modes which shows only one mode active q_2 .

Figure 10 clearly shows that the residue signal is deferent from zero in the time interval [0.11 s 0.21 s] due to blocking the switch $u_3 = 0$.

3.5. Non-Transition

We consider blocking the functioning of the system in mode q_6 from $t = 0.1$ s to $t = 0.2$ s. The evolution of the variables of state and output voltage V_s are shown respectively in Figure 11 and Figure 12.

Figure 13 indicates that the residue is not zero in the interval from $t = 0.1$ s to $t = 0.2$ s, indicating the appearance of the default due to no transition.

Figure 14 shows the state of each cell during the non-transition fault and therefore shows cell 2 and blocked temporarily 0. Figure 15 presents the state of the switches, which shows blocking the

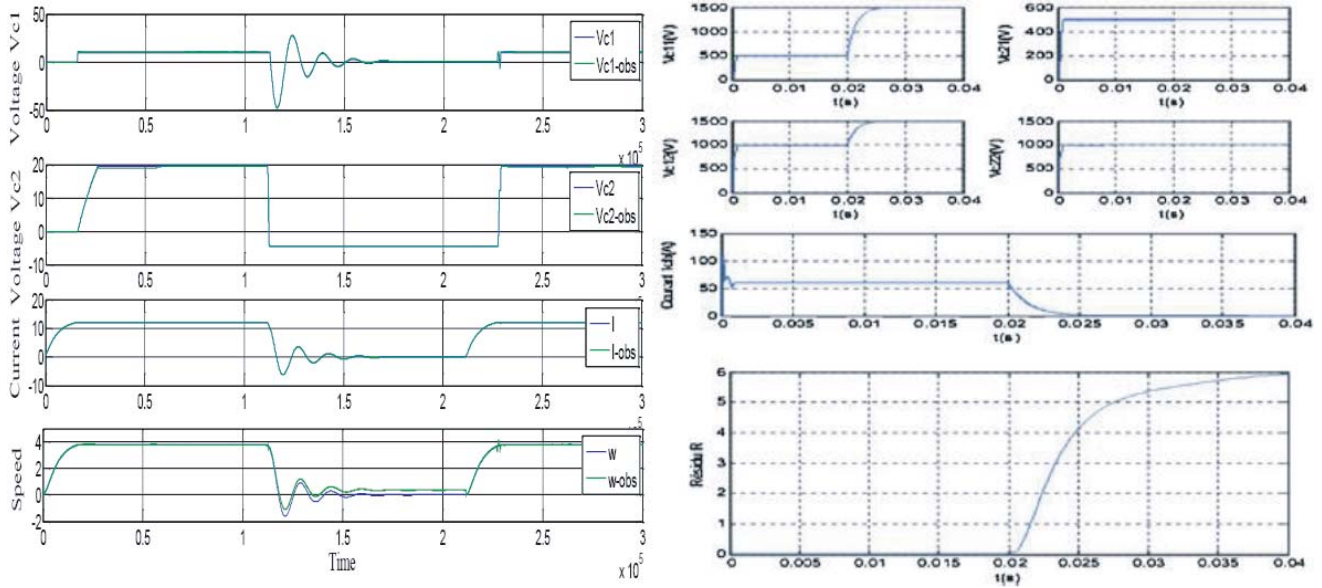


Figure 7. Evolution of the state variables of the converter due to blocking the switch $u_3 = 0$. We notice that we obtained the same results as the results obtained on [28] showing in the next figure.

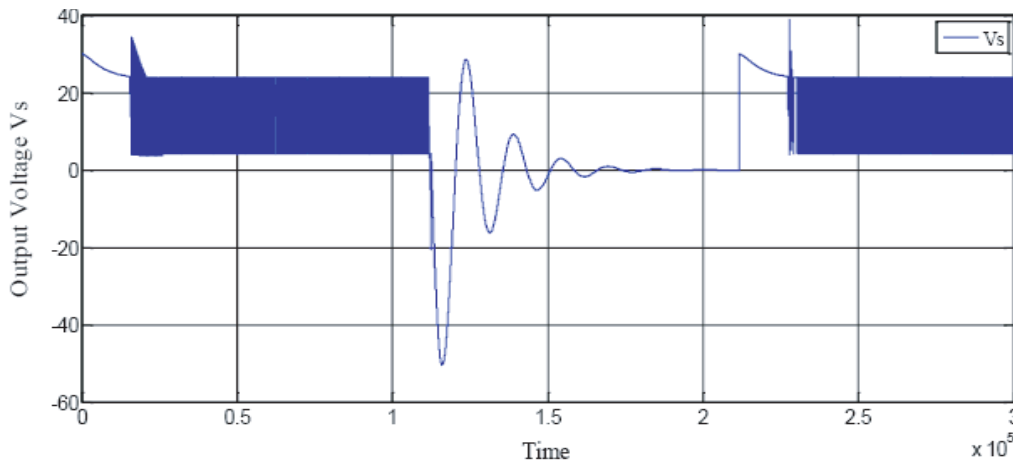


Figure 8. Evolution of the output voltage V_s due to blocking the switch $u_3 = 0$.

functioning of the system in mode q_6 indicated by the states of $u_1 = 1, u_2 = 0, u_3 = 1$, in the time interval $[0.11 \text{ s } 0.21 \text{ s}]$ (blocking mode does not mean blocking switches).

3.6. Transition to a Non-Successor Mode

Each transition $T_{ij} \in H$ is associated with a condition of crossing. The transition cannot be crossed if the condition is true.

There are two possible cases for this fault: Transition to a non-successor mode with blocking and transition to a non-successor mode without blocking.

- Transition to a non-successor mode with switch blocking
 For fault transition from mode q_8 to mode q_2 which is not successor at $t = 0.1 \text{ s}$, the results the functioning the system are shown in Figures 16 and 17.
 Figure 18 indicates that the residue is not zero on the interval from $t = 0.1 \text{ s}$ to $t = 0.2 \text{ s}$, indicating the appearance of the default due to a transition to mode not successor.

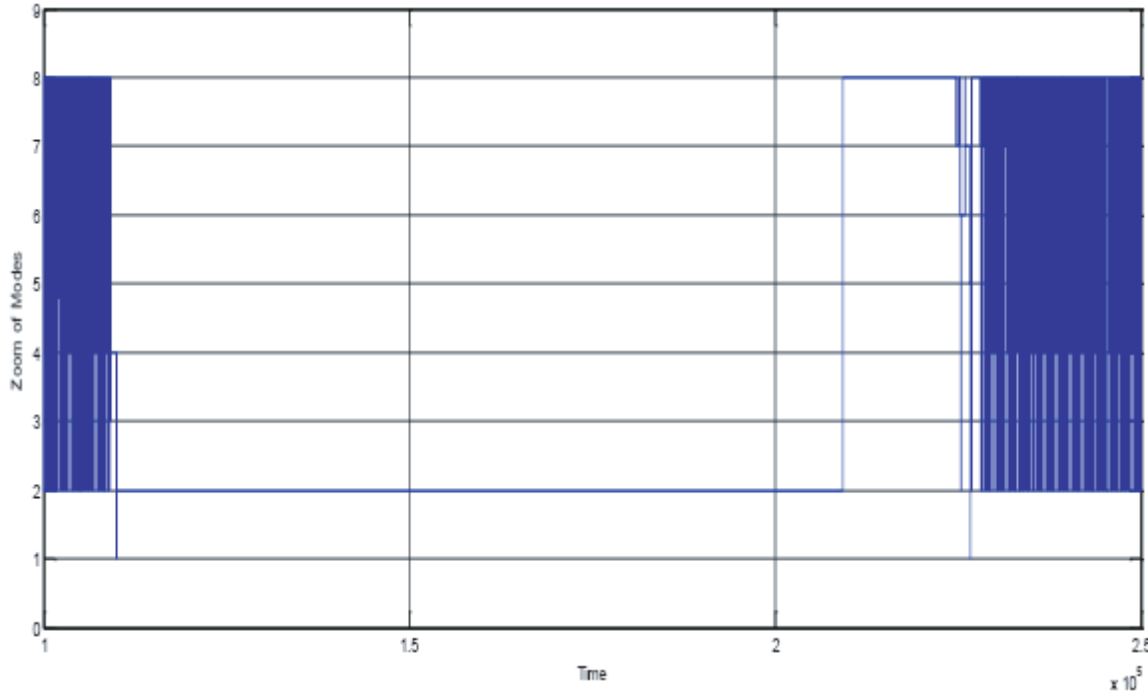


Figure 9. Present a zoom of the evaluation of modes witch shows only one mode active q_2 in interval of time $[0.11\text{ s } 0.21\text{ s}]$.

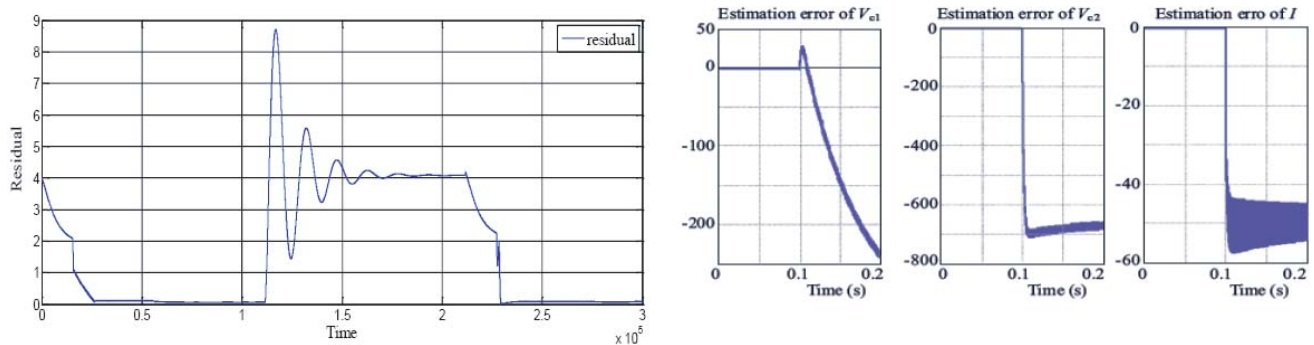


Figure 10. Evolution of the residue due to blocking the switch $u_3 = 0$. When the switch u_3 is blocked in 0 we have same results as [25].

Figure 19 presents the state of the switches, which shows the transition to not successor at $t = 0.1254\text{ s}$, indicated by the change of more than one state of switches from q_8 : $u_1 = 1, u_2 = 1, u_3 = 1$ to q_2 : $u_1 = 1, u_2 = 0, u_3 = 0$.

- Transition to a non-successor mode without blocking

It is the case where the fault is a fault of condition of transition from mode q_7 to mode q_6 . Figure 20 shows the evolution of variables of state of the converter in the event of fault transition. The changes of the state variables are shown in Figure 21 and the output variable in Figure 22.

The residual signal presented in Figure 23 shows that there is a fault in the system functioning in the time interval $[0.11\text{ s } 0.21\text{ s}]$.

We can see clearly that the localization fault of switches does not detect any problem of function where both of the residual signal and detection signal show that there is a fault. Then we find a solution to this problem by creating a localization bloc that can detect and localize any possible fault of transition.

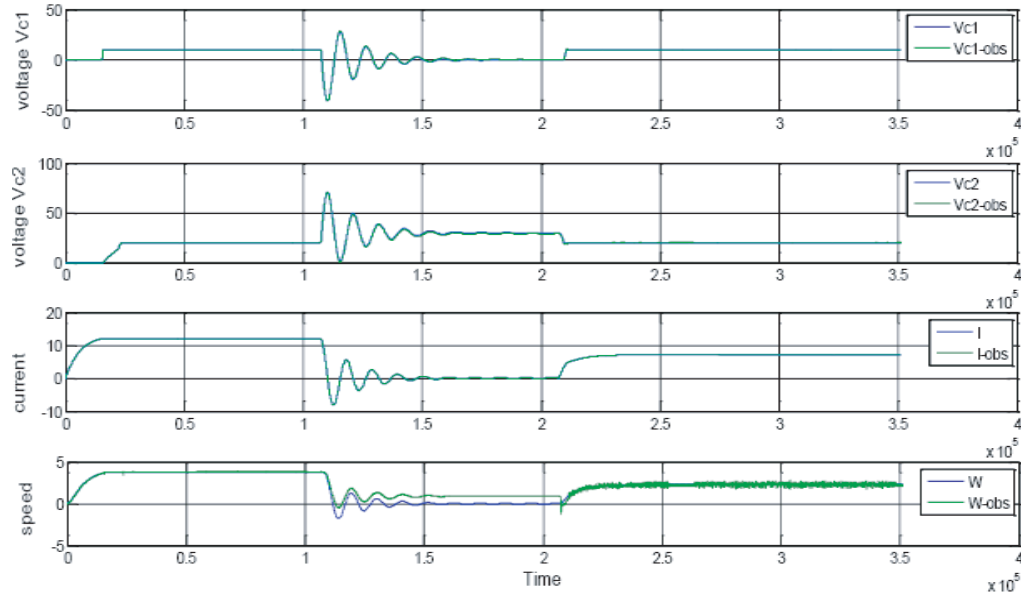


Figure 11. Evolution of the variables of state during the fault.

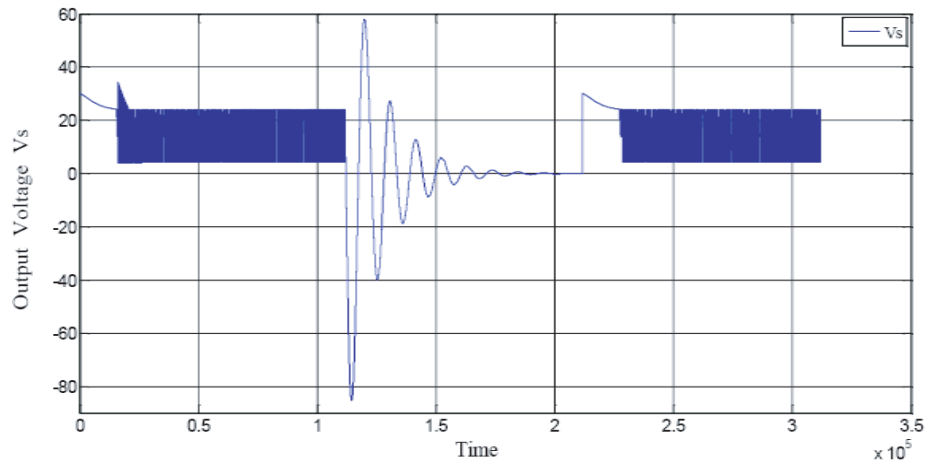


Figure 12. Evolution of output voltage V_s .

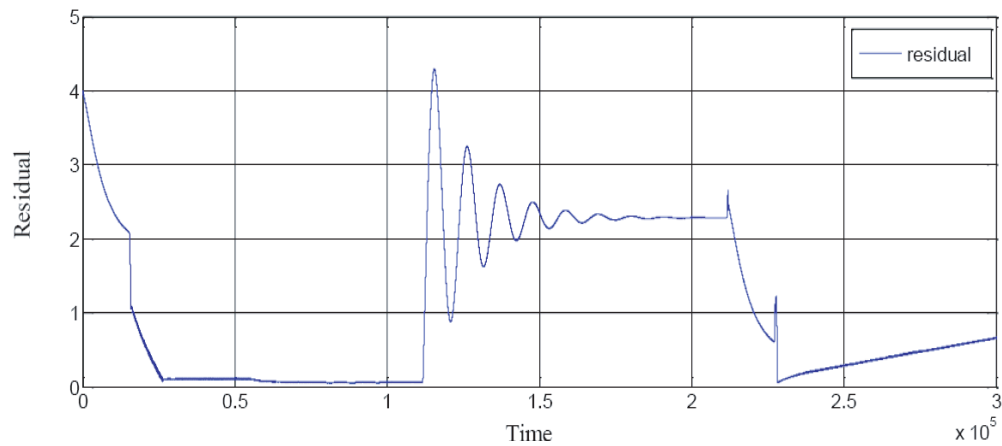


Figure 13. Evolution of the residual signal in the event of fault non transition.

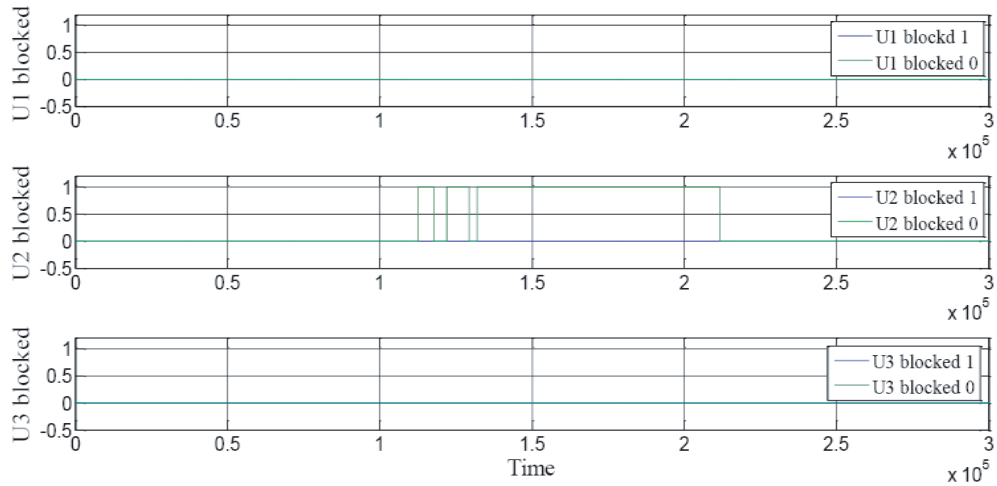


Figure 14. State of switches.

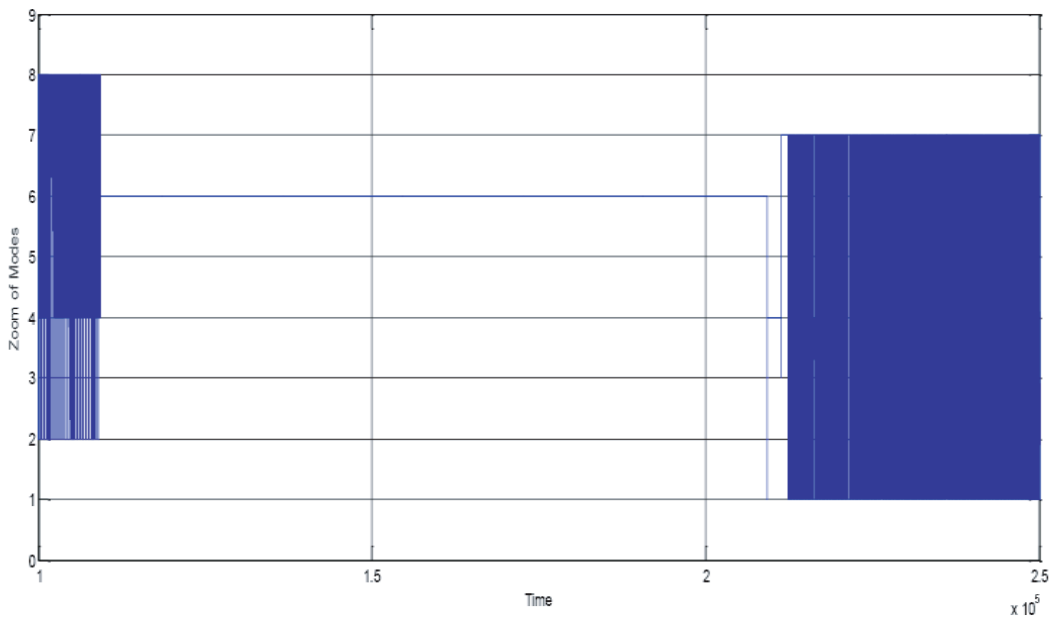


Figure 15. Present a zoom of the evaluation of modes which shows only one mode active q_6 in interval of time $[0.11 \text{ s } 0.21 \text{ s}]$.

With this block of detection of fault transition we can find that there is a fault transition in mode 6, but the problem is how we can find the non-successor mode that sends the transition.

To find a solution, we create a block which checks all origins of coming transition and compare with the successors modes; if the coming transiting is from a successor mode, the signal is equal to 0, and the block reserves the origin mode of coming transition, else equal to 1 and also reserves the origin mode of the coming transition. By this signal we can find the origin of the fault transition.

With Figure 24 we can find exactly where is the fault transition in this case, and mode 7 is the non-successor mode.

With this signals we can detect, localize, and find where the fault is in the system if it exists. In this article, we inject different types of fault and observe that with the detection and localization blocks we can detect and localize any possible fault whatever its nature.

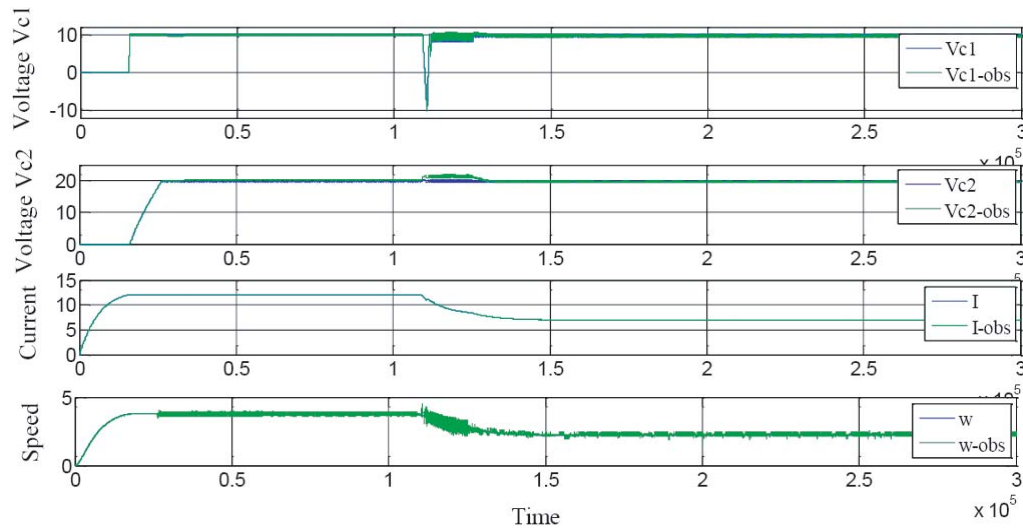


Figure 16. Evolution of the variables of state of the converter in the event of fault transition.

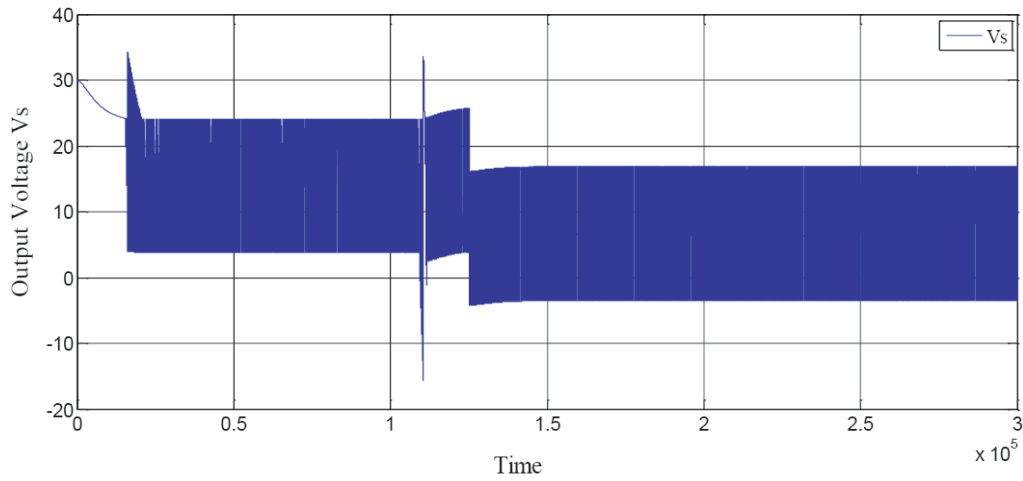


Figure 17. Evolution of V_s the output voltage.

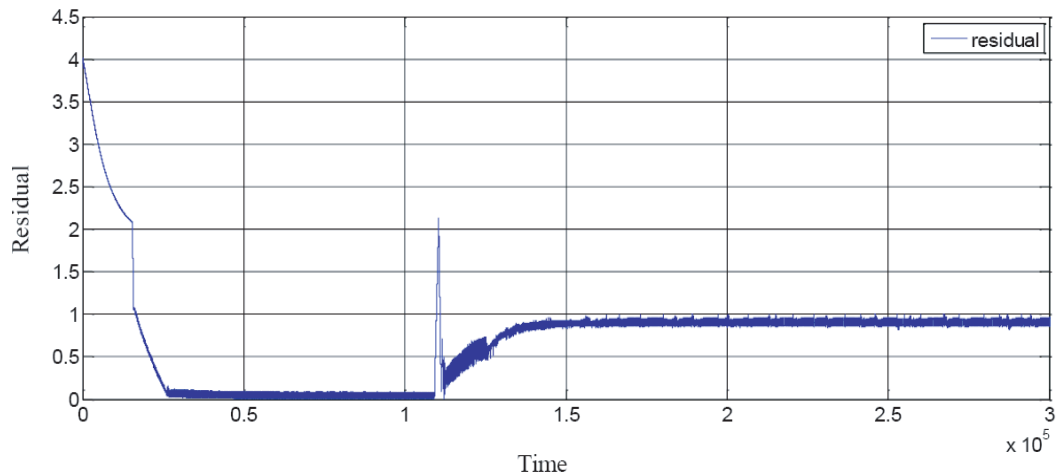


Figure 18. Evolution of the residue in the event of fault transition.

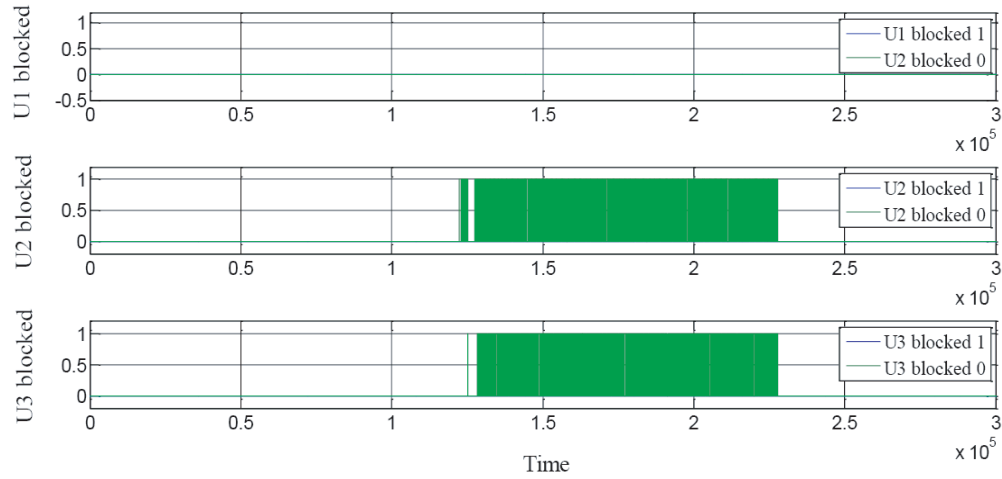


Figure 19. State of switches.

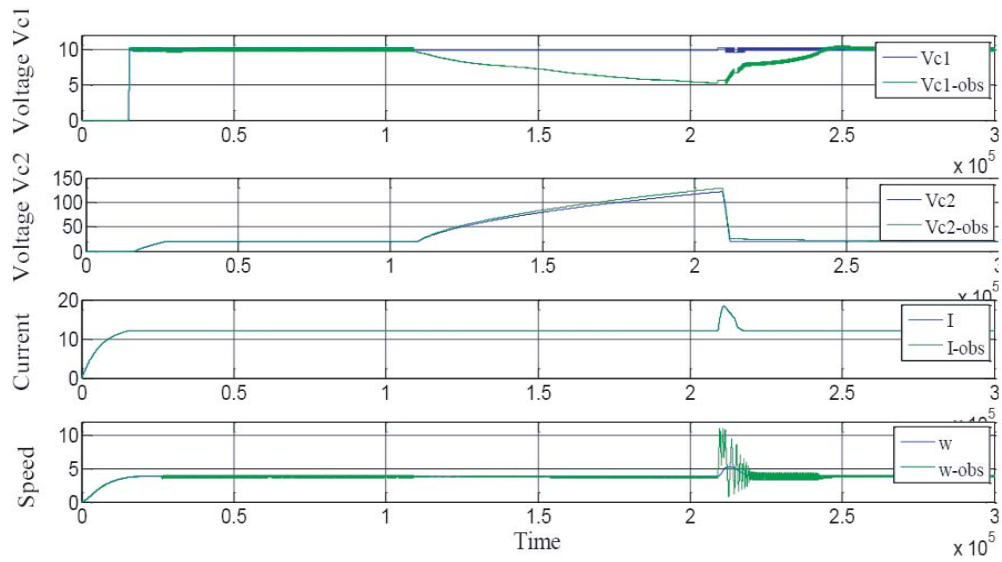


Figure 20. Evolution of the variables of state of the converter in the event of fault transition.

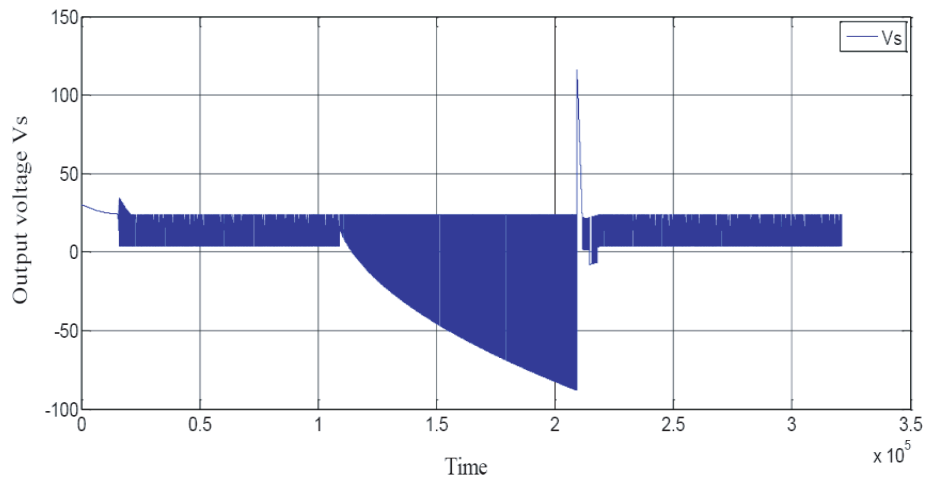


Figure 21. Evolution of the output voltage in the event of fault transition.

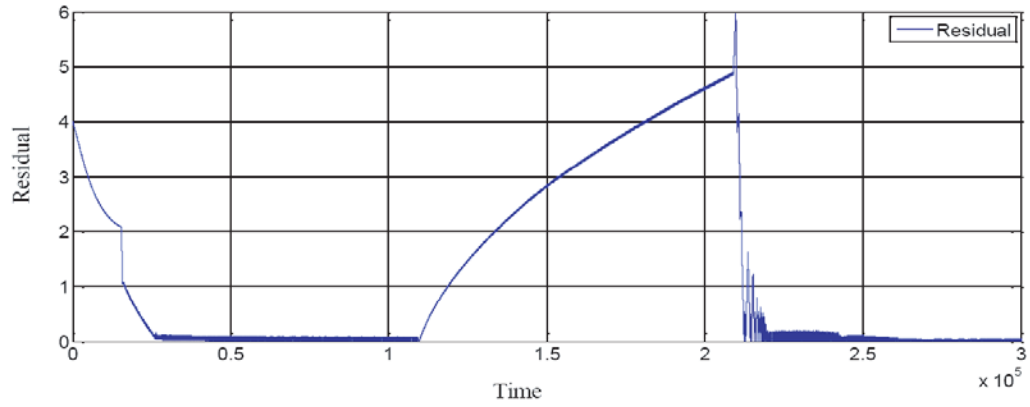


Figure 22. Evolution of the residue signal in the event of fault transition.

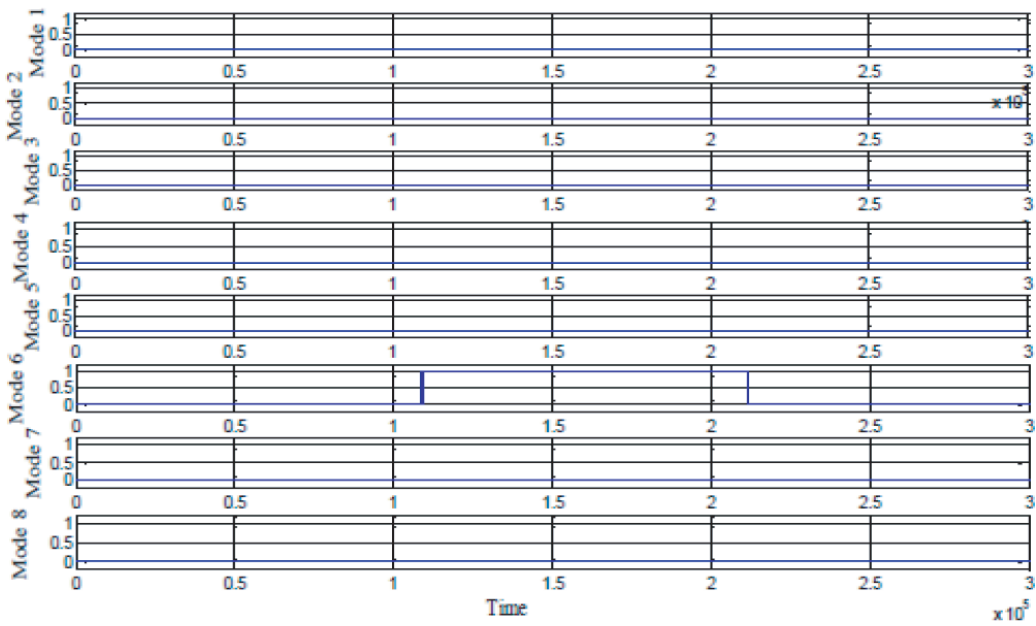


Figure 23. Localization signal of transitions in the event of fault transition.

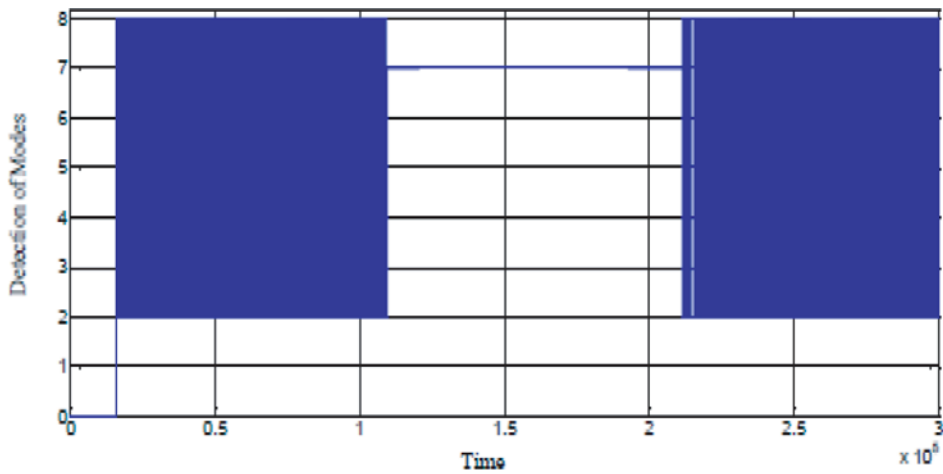


Figure 24. The detection of modes signal of modes in the event of fault transition.

4. CONCLUSION

In this paper, a hybrid modeling of the converter of three cells associated with DC motor is proposed. Then an observer based on sliding mode is presented to estimate the voltages of the capacitors C_1 and C_2 . We discuss a hybrid approach for fault diagnosis which is based on the generation of residues with an observer. The simulation results validate the used method. Furthermore, it has been shown that the DC motor speed coupled to the multicell consider can be estimated with an acceptable error because the dynamics of the electrical part (multicell chopper) is much faster than that of the mechanical parts (DC motor). Some additional results show an observer for partial state observation and the conditions under which it can be designed.

REFERENCES

1. Erickson, R. and D. Maksimovic, *Fundamentals of Power Electronics*, 2nd Edition, Kluwer Academic Publishers, Dordrecht, The Netherlands, 2001.
2. Meynard, T. A., H. Foch, P. Thomas, J. Courault, R. Jakob, and M. Nahrstaedt, "Multicell converters: Basic concepts and industry applications," *IEEE Transactions on Industrial Applications*, Vol. 49, No. 5, 955–964, 2002.
3. Tolbert, L. M. and F. Z. Peng, "Multilevel converters for large electric drives," *Proceedings of the IEEE APEC'98*, 530–536, Anaheim, USA, 1998.
4. Ladoux, P., M. Machmoum, and C. Batard, "Harmonic currents compensation for 1.5 kV DC railway substations," *International Review of Electrical Engineering*, Vol. 4, No. 3, 380–391, June 2009.
5. Stala, R., S. Pirog, A. Mondzik, M. Baszynski, A. Penczek, J. Czekonski, and S. Gasiorek, "Results of investigation of multicell converters with balancing circuit," *IEEE Trans. Industrial Electronics*, Vol. 56, No. 7, 2620–2628, July 2009.
6. Sadigh, A. K., S. H. Hosseini, and G. B. Gharehpetian, "Double flying capacitor multicell converter based on modified phase-shifted pulsewidth modulation," *IEEE Transactions on Power Electronics*, Vol. 259, No. 6, 1517–1526, June 2010.
7. Defoort, M., M. Djemai, and J. Van Gorp, "Sliding mode control of switching electrical power converters associated to an inductive load," *IFAC World Congress*, 2011.
8. Gateau, G., M. Fadel, P. Maussion, R. Bensaid, and T. Meynard, "Multicell converters: Active control and observation of flying capacitor voltages," *IEEE Transactions on Industrial Electronics*, Vol. 49, 998–1008, 2002.
9. Baja, M., D. Patino, H. Cormerais, P. Riedinger, and J. Buisson, "Hybrid control of a three-level three-cell DC-DC converter," *Proceedings of the IEEE American Control Conference*, 5458–5463, New York City, USA, 2007.
10. Ghanes, M. and J. P. Barbot, "On sliding mode and adaptive observers design for multicell converter," *Proceedings of the IEEE American Control Conference*, 2134–2139, St Louis, Missouri, USA, 2009.
11. Djemai, M., K. Busawond, K. Benmansoure, and A. Marouf, "High-order sliding mode control of a DC motor drive via a switched controlled multi-cellular converter," *International Journal of Systems Science*, Vol. 42, No. 11, 1869–1882, 2011.
12. Meradi, S., K. Benmansour, M. Tadjine, M. S. Boucherit, "Fault hybrid diagnosis cells in four levels flying capacitors multicell converter," *International Conference of Maintenance, Management, Logistics and Electronics*, Oran, Algeria, 2012.
13. Meradi, S., K. Benmansour, K. Herizi, M. Tadjine, and M. S. Boucherit, "On hybrid observability design for multi-cellular four quadrants dc-dc converter," *International Symposium on Environment Friendly Energies and Applications*, 2012.
14. Van Gorp, J., M. Defoort, and M. Djemai, "Binary signals design to control a power converter," *50th IEEE Conference on Decision and Control*, 2011.

15. Liu, J., S. Laghrouche, M. Harmouche, and M. Wack, "Adaptive-gain second-order sliding mode observer design for switching power converters," *Journal of Control Engineering Practice*, Vol. 30, 124–131, 2014.
16. Defoort, M., M. Djemai, T. Floquet, and W. Perruquetti, "Robust finite time observer design for multicellular converters," *International Journal of Systems Science*, Vol. 42, No. 11, 1859–1868, 2011.
17. Silva, E. I., B. McGrath, D. Quevedo, and G. Goodwin, "Predictive control of a flying capacitor converter," *IEEE American Cont. Conf.*, 2007.
18. Benmansour, K., J. De Leon, and M. Djemai, "Adaptive observer for multi-cell chopper," *Second International Symposium on Communications, Control and Signal Processing*, March 13–15, 2006.
19. Bejarano, F. J., M. Ghanes, and J.-P. Barbot, "Observability and observer design for hybrid multicell choppers," *International Journal of Control*, Vol. 8, No. 3, 617–632, 2010.
20. Utkin, V., *Sliding Modes in Control and Optimisation*, Springer-Verlag, Berlin, 1992.
21. Ghanes, M., F. Bejarano, and J. P. Barbot, "On sliding mode and adaptive observers design for multicell converter," *American Control Conference*, 2009.
22. Cheng, P.-J., C.-H. Cheng, and C.-C. Tung, "Design of DC motor's torque control using DSP," *Journal of Information and Optimization Sciences*, Vol. 30, No. 6, 1197–1207, 2009.
23. Trabelsi, M. A., "Modélisation et commande directe d'un convertisseur multi niveau monophasé," *JCGE'08 Lyon*, 2008.
24. Ben Said, S., K. Ben Saad, and M. Benrejeb, "Sliding mode control for a multicell converters," *CEIT'13*, Sousse, Tunisie, June 4, 2013.
25. Benzineb, O., F. Taïbi, T. Meriem, L. Kirati, M. S. Boucherit, and M. Tadjine, "Control and fault diagnosis based sliding mode observer of a multicellular converter: Hybrid approach," *Journal of Electrical Engineering*, Vol. 64, No. 1, 20–30, 2013.
26. Ramadge, P. J., "Observability of discrete event-systems," *Proceedings of 25th Conference on Decision and Control*, 1108–1112, Athens, Greece, 1986.
27. Benzineb, O., F. Taïbi, M. E. H. Benbouzid, M. S. Boucherit, and M. Tadjine, "Multicell converters hybrid sliding mode control," *International Review on Modelling and Simulations*, Vol. 4, No. 4, 1396–1403, 2011.
28. Meradi, S., K. Benmansour, K. Herizi, M. Tadjine, and M. S. Boucherit, "Sliding mode and fault tolerant control for multicell converter four quadrants," *Elsevier Electric Power Systems Research*, Vol. 95, 128–139, 2013.
29. Belkhiat, D. E. C., N. Manamanni, N. Messai, and M. Djemai, "Fault detection & isolation for a class of hybrid systems: A dedicated switched robust observer scheme," *2012 20th Mediterranean Conference on Control & Automation (MED)*, 984–989, Barcelona, 2012.
Van Gorp, J., A. Giua, M. Defoort, M. Djemai, and S. Paganelli, "Fault detection and isolation for a class of switched systems," *IEEE Transactions on Power Electronics*.
30. Meynard, T., H. Foch, P. Thomas, J. Courault, R. Jakob, and M. Nahrstaedt, "Multi-cell converters: Basic concepts and industry applications," *IEEE Transactions on Industrial Application*, Vol. 49, No. 5, 955–964, 2002.
31. Kang, W., J. Barbot, and L. Xu, "On the observability of nonlinear and switched systems," *Lecture Notes in Cont. and Inf. Sciences*, Springer Berlin, 2009.